High-temperature induced ferromagnetism on γ-Fe precipitates in FeCu solid solutions

Pedro Gorria, David Martínez-Blanco, Jesús A. Blanco, and María José Pérez
Departamento de Física, Universidad de Oviedo, 33007 Oviedo, Spain

Antonio Hernando
Instituto de Magnetismo Aplicado, UCM-RENFE, 28230 Las Rozas, Madrid, Spain

Luis Fernández Barquín
Departamento CITIMAC, F. Ciencias, Universidad de Cantabria, 39005 Santander, Spain

Ronald I. Smith
ISIS Facility, Rutherford Appleton Laboratory, Chilton, Didcot, Oxon OX11 0QX, United Kingdom
(Received 26 August 2004; revised manuscript received 12 April 2005; published 1 July 2005)

Experimental results of magnetization and neutron diffraction in the temperature range 300–1100 K evidence an anomalous high-temperature irreversible magnetic behavior on metastable FeCu solid solutions. When the temperature is increased above 500 K, a segregation process takes place in the as-milled sample which gives rise to the appearance of Fe (bcc) and Cu (fcc) phases. Further heating shows that the magnetization at 850 K falls down due to the temperature dependence of the bcc-Fe magnetization and the onset of the α-γ martensite transformation. The temperature of this martensite phase transition (1020 K) is more 100 K lower than that of pure α-Fe (1183 K). On cooling from high temperatures (1100 K), the magnetization does not appreciably increase its value until the temperature is lowered below 900 K, showing a broad hysteresis between the forward (warming) and the reverse (cooling) transformations. Apart of the above mentioned bcc-Fe and fcc-Cu phases, on cooling, a small amount of isolated γ-Fe precipitates ($\approx 5\,\%$) is detected. Further heating above 600 K show a large magnetization enhancement, reaching a value 50% higher with respect to the value measured at room temperature. During cooling from 1100 K the maximum value of magnetization is not recovered. The origin of this anomalous high temperature magnetic behavior is explained on the basis of strong magnetovolume instabilities in γ-Fe. Furthermore, the thermal expansion coefficient of the γ-Fe precipitates ($21-23\times10^{-6}$ K^{-1}), obtained from the neutron-diffraction patterns, is in excellent agreement with that calculated theoretically ($20-24\times10^{-6}$ K^{-1}, along the studied temperature range 300–1100 K). This fact is a signature of an anti-Invar behavior in γ-Fe precipitates that could explain this surprising magnetic response.

DOI: 10.1103/PhysRevB.72.014401 PACS number(s): 75.50.Bb, 61.12.−q, 64.60.My, 75.30.Kz

I. INTRODUCTION

The magnetism of iron and its binary metallic alloys is a subject of huge interest and research effort, because of both basic significance and potential practical applications.[1] Nevertheless, some issues, especially those related with iron in a face centered cubic (fcc) lattice, the so-called γ-Fe, are still a hot topic of discussion at the present.[2,3] Total-energy band calculations predict a very rich and complex magnetic phase diagram,[4,5] including the presence of large moment-volume instabilities,[6–8] responsible for the existence of Invar and anti-Invar behaviors. Contrary to the Invar effect, where a nearly zero thermal expansion is observed in some magnetically ordered materials, other systems exhibits, in the paramagnetic state, an anomalous thermal expansion larger than that described by a Grüneisen lattice. The term anti-Invar was coined for such a behavior.[9] On the other hand, recent "*ab initio*" calculations have confirmed the phenomenological model proposed by Weiss in the 1960's[10] based on two spin-electronic γ states. These two discrete states are known as a "low-spin low-volume" state (LS), with a lattice parameter around 3.5 Å, and a "high-spin high-volume" state (HS), with a lattice parameter above 3.6 Å. The estimated value for the Fe magnetic moment μ_{Fe} in the LS state is below $1\mu_B$, while for the HS state μ_{Fe} can reach to values over $2.5\mu_B$.

Nowadays, it is recognized that the γ-Fe is located at a *crossing point* of ferromagnetic (HS) and antiferromagnetic states, and its magnetism depends very much on the atomic volume,[11,12] being assumed that the magnetic behavior of γ-Fe at 0 K is antiferromagnetic.[13] However, it is well known that γ-Fe is only stable at high temperatures (above 1183 K), it being very difficult to stabilize this phase at room temperature. The usual route to achieve this task is the substitution of Fe atoms in a simple lattice with a fcc structure, such as those offered by some pure metals (Ni, Pt, Pd, Cu).[9] But still, two basic conditions are needed if the study of γ-Fe magnetism is pursued: (i) a lattice parameter in the range $a\approx 3.50-3.65$ Å and (ii) the fcc matrix where Fe atoms should be located must be nonmagnetic. The best candidate that fulfills both these requirements is Cu ($a=3.615$ Å). However, the miscibility of Cu and Fe is very low under equilibrium conditions, and only modern synthesis procedures such as deposition techniques[14,15] allows stabilizing, even at low temperatures, γ-Fe precipitates in a Cu matrix as well as epitaxial films on a Cu substrate. Alternatively, mechanical alloying[16–18] offers the possibility to obtain bulk fcc-FeCu metastable solid solutions in *large* quantities and with a *wide* compositional range (up to 65 at. % in Fe).

The fcc-FeCu metastable materials show ferromagnetism for Fe concentrations above 15 at. % and the lattice param-

eter being larger ($a > 3.63$ Å) than that of pure fcc-Cu (3.615 Å).[19–21] In special conditions, large magnetovolume effects can be observed, giving rise to macroscopic Invar behavior.[22] By contrast, small amounts of γ-Fe precipitates in a Cu matrix exhibit antiferromagnetic order below 70 K, with $\mu_{\mathrm{Fe}} \sim 0.5\mu_B$ at 0 K.[23] Because of the metastable nature of these materials, heating above 500 K produces a well-known segregation process,[16,17] which is concluded around 800 K. Then, the system transforms into body centered cubic (bcc) and fcc phases (which are Fe- and Cu-rich phases, respectively) plus a small amount of another fcc (Fe-rich) or γ-Fe phase.[24,25] Using magnetization measurements as well as Mössbauer spectroscopy at low temperature, an intense search for magnetic order in these isolated γ-Fe precipitates has been performed.[26,27] However, no order was found even below 10 K. This result can be understood taking into account that the lattice parameter of this γ-Fe phase (below 3.6 Å) is lower than that expected for HS state.

After a previous work (see Ref. 22) in which we have determined the magnetic phase diagram of mechanical alloyed Fe-Cu, in this article we present a detailed structural and magnetic characterization of the Fe-Cu solid solutions at high temperatures (300–1100 K) focused mainly on the Cu-rich concentration side. The aim is to study the temperature range stability and coexistence of both α-Fe and γ-Fe phases and the magnetic response of each phase.

II. EXPERIMENTAL DETAILS

Three samples of Fe_xCu_{100-x} with $x=16$, 44, and 65 were obtained in powder form using high-energy ball milling. The magnetic measurements were performed (under an applied magnetic field of 1 kOe) using a Faraday susceptometer, which allows the mounting of a furnace able to reach as high as 1100 K, located at the University of Oviedo. On the other hand, independently of the magnetization measurements, neutron thermodiffraction experiments were performed on the Polaris time-of-flight diffractometer (ISIS facility, Rutherford Appleton Laboratory, UK). Diffraction patterns were collected every 10 K in order to follow all the possible structural changes during heating, while on the cooling process the temperature was not controlled. The wide d-spacing range measured (0.35–3.00 Å in the highest resolution backscattering detector bank), allows us to perform high quality Rietveld refinements (using the FULLPROF package)[28] of the crystallographic structures because at least 35 reflections for each of the crystalline phases are present. The reliability factors are not exceeding 3–4 %. Both magnetic measurements and thermodiffraction experiments were carried out independently at a controlled heating rate of 10 K/min, and under inert atmosphere in order to avoid oxidation of the samples.

III. RESULTS AND DISCUSSION

A. Segregation of α-Fe and α-γ transformation

To follow adequately the discussion of the magneto-structural processes involved here, it is necessary to observe simultaneously the results presented in Fig. 1 (in which the magnetization, M, in the range $300\ \mathrm{K} < T < 1100\ \mathrm{K}$ is shown), 2, and 4 (in which the relevant diffraction peaks are shown). The fcc-$Fe_{16}Cu_{84}$ solid solution exhibits Invar ferromagnetic behavior, with a Curie temperature T_C below 150 K. In Fig. 1, on heating, above $T_S^i = 530$ K a progressive increase in M is observed due to the segregation of Fe atoms from the fcc-FeCu lattice leading to the formation of a bcc-Fe-rich phase [see Fig. 2(b)]. The increase in M finishes at around $T_S^f = 780$ K indicating the end of the segregation process. For higher temperatures, the value of M remains almost constant for about 40 K and then falls down rapidly above 835 K. However, M does not drop to vanishing values, but features a shoulder beginning above 880 K with a decreasing tendency when the temperature increases, this time, to vanishing values. This suggests that the T_C of the bcc-Fe phase is below 990 K, lower than the expected value of $T_C = 1043$ K for pure α-Fe. The behavior for $T > 835$ K (warming up) can be ascribed to two combined effects: on the one hand, a structural effect [reflected in the $M(T)$ curve] related to the onset of the martensite-austenite α-γ transformation (MA) (starting at $A_s \approx 835$ K and being complete at the finish temperature $A_f \approx 1020$ K), occurring at lower temperatures than expected for pure α-Fe [$T_{\mathrm{MA}}(\alpha\text{-Fe}) = 1183$ K]; and on the other hand, a magnetic contribution, with a usual decreasing $M(T)$ curve towards T_C for α-Fe.

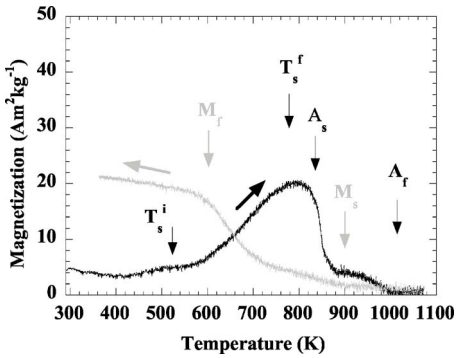

FIG. 1. Magnetization vs temperature $M(T)$, curves for the fcc-$Fe_{16}Cu_{84}$ solid solution for the first heating (black) and cooling (grey) processes in the as-milled sample. Vertical arrows indicate the initial (T_S^i) and final (T_S^f) segregation temperatures, the initial (A_s) and final (A_f) Martensite-Austenite transformation temperatures and the initial (M_s) and final (M_f) Austenite-Martensite transformation temperatures. Note that magnetization scale is set adequately to be compared with those of Figs. 5 and 7.

In the reverse transformation, i.e., on cooling from highest (1080 K) temperature in $M(T)$, M remains almost zero down to around 900 K, which is a clear evidence of a typical thermal hysteretical behavior on heating-cooling procedures for the MA transition of other Fe alloys.[29] These features rule out the existence of another ferromagnetic phase that could coexist with the Fe-rich bcc phase. This is also confirmed by the already presented neutron patterns shown in Fig 2. Focusing now our attention on the neutron-diffraction data taken every 10 K, all the structural transformations undergone by the as-milled solid solution $Fe_{16}Cu_{84}$ have been monitored. Only a restricted d-spacing range is shown for clarity, where the most intense reflections of the fcc and bcc phases are observed. It is worth mentioning the considerable

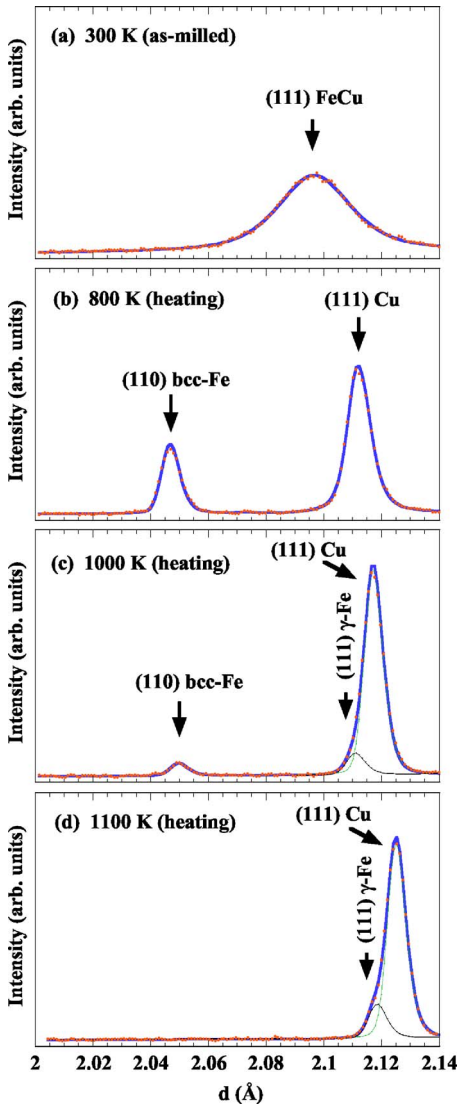

FIG. 2. (Color online) Neutron-diffraction patterns obtained at selected temperatures during the heating processes for the fcc-$Fe_{16}Cu_{84}$ solid solution. Only the relevant d range is shown for clarity. The lines represent the result of a Rietveld refinement.

width of the reflections, which are noticeably broader at lower temperatures, Figs. 2(a) and 2(b). This is due to a decrease of particle size (reaching sometimes the nanometer scale) and microstrain effects (usually below 1%), which are typical of as-milled granular alloys.[30] On heating the peaks sharpen considerably [Figs. 2(b)–2(d)] due to structural relaxation processes in the metastable as-milled alloys. At 800 K two peaks are evident, one corresponding to the (110) reflection of the segregated bcc-Fe-rich phase and the other stems from the (111) reflection of the fcc-Cu-rich phase [see Fig. 2(b)]. However, at $T=1000$ K [see Fig. 2(c)], the (110) reflection of the bcc phase decreases markedly, being zero around 1020 K, more than 100 K below the MA (α-γ) transformation for pure Fe. This decrease of the temperature at which the α-γ transformation takes place is due to small amount of Cu dissolved in the segregated bcc-Fe phase, in a similar way as in bcc-FeNi alloys.[29] From Fig. 2(c), it is also worth noting that two fcc phases coexist at 1000 K [the (111) reflection shows a small shoulder in the left hand edge of the peak, at shorter d spacing]: one Cu rich and the other Fe rich. This fact indicates that the α-γ transformation for the bcc-Fe phase has taken place, and discards a possible re-agregation of Fe atoms into the Cu phase. Finally, the coexistence of both fcc γ-Fe and Cu phases at 1100 K is presented in Fig. 2(d). The temperature dependence of the integrated intensity associated with the reflection (110) of the bcc-Fe phase is shown in Fig. 3. It is remarkable that a similar trend is followed by the magnetization (see Fig. 1) and the neutron integrated intensity (see Fig. 3) on heating above 500 K, confirming that the increase of magnetization is proportional to the amount of such a phase.

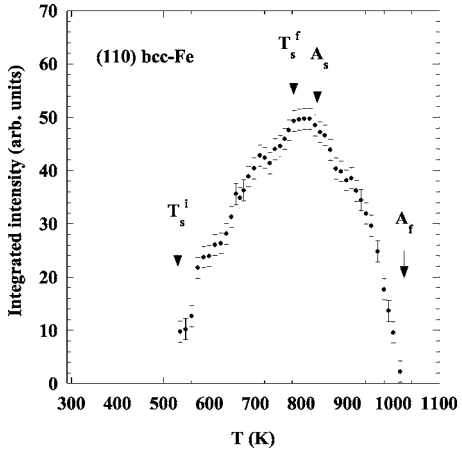

FIG. 3. Temperature dependence of the integrated intensity of the (110) reflection of bcc-Fe-rich phase segregated from the fcc-$Fe_{16}Cu_{84}$ solid solution during the first heating process.

During cooling down from 1100 K (see Fig. 4) to room temperature (RT), the reflection (110) associated with the ferromagnetic bcc-Fe phase does not appear again until the temperature is lowered below 920 K. The presence of this phase leads to the increase of the magnetization below this temperature [the reverse α-γ transformation starts at $M_s=900$ K, being finished at $M_f=600$ K on cooling (as can be seen in Fig. 1) as the temperature is decreased]. The further increase of the magnetization on decreasing temperature can be related to the regular behavior of the magnetization of bcc-Fe. Furthermore, a clear shoulder associated with the existence of a peak with a $d<2.08$ Å is seen. This is fitted with a contribution ascribed to a Fe-rich phase with fcc structure [see Figs. 4(b)–4(d)]. Finally, from the neutron pattern collected at RT after cooling from 1100 K, only reflections corresponding to three crystalline phases fcc-Cu, bcc-Fe, and γ-Fe are present.

We have estimated the amount of bcc-Fe at the end of the segregation process $T_S^f=780$ K from the Rietveld refinement of the neutron diffraction pattern [Fig. 2(b)], giving a value around 15%. The same percentage is obtained for the γ-Fe phase at high temperatures [Fig. 2(d)], while the volume fractions for α- and γ-Fe at RT after cooling from 1100 K [Fig. 2(d)] are ~10% and ~5–6 % respectively. Also, magnetic measurements give approximately the same relative percentages attending to the magnetization values (assuming 217 A m^2 kg^{-1} for pure iron at RT, and above 250 A m^2 kg^{-1}

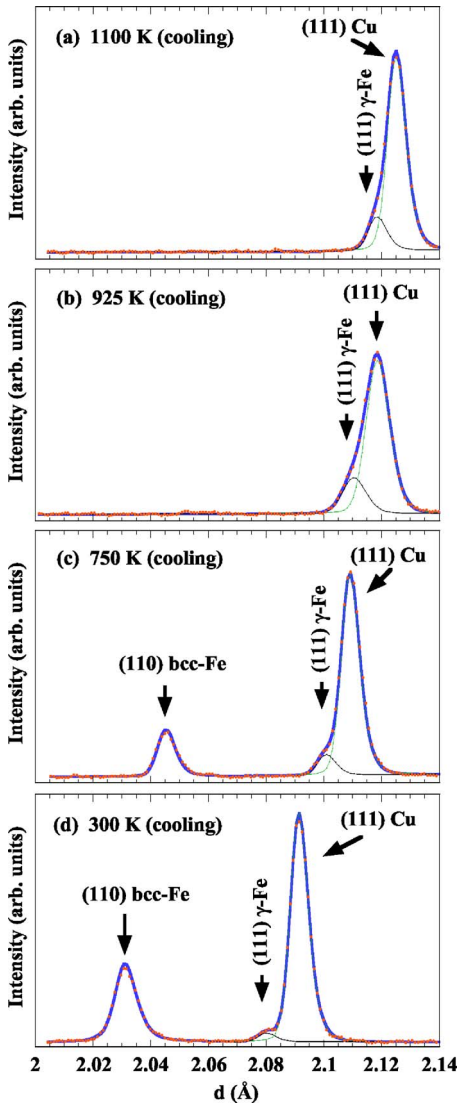

FIG. 4. (Color online) Neutron-diffraction patterns obtained at selected temperatures during the cooling processes for the fcc-$Fe_{16}Cu_{84}$ solid solution. Only a restricted d range is shown for clarity. The data were fitted (lines) using Rietveld refinement. Compare this with patterns shown in Fig. 2.

for γ-Fe which is equivalent to a value for the magnetic moment over $2.5\mu_B$). In this way, neutron diffraction confirms early results reported in the literature, obtained from Mössbauer spectroscopy and transmission electron micrsocopy,[17,25,26,31] which claim for a small amount of nonmagnetic γ-Fe precipitates that remain isolated between fcc-Cu and bcc-Fe majority phases. In addition to that, and if we go back to Fig. 1, we can see that the magnetization value at RT after cooling is slightly lower than the maximum magnetization value reached during the first heating, indicating the nonmagnetic nature of the isolated γ-Fe phase at RT. Hence, it is possible to produce a significant (6% in weight quantities) amount of bulk γ-Fe in using controlled warming procedure.

B. Second and subsequent heating and cooling cycles

The most striking behavior takes place in the subsequent heating processes; see Fig. 5. An abrupt increase in the magnetization is observed above 600 K, reaching a value of 50% larger than that at RT. Further heating provokes a decrease of magnetization above 800 K. During the cooling process from 1075 K the values of magnetization (at the maximum 32 A m^2 kg^{-1}) reached during heating are not recovered, although the values at RT are the same (22 A m^2 kg^{-1}). Subsequent heating (up to 1075 K) and cooling (down to RT) procedures show overlapping $M(T)$ curves to those in Fig. 5. To investigate further this striking behavior we have studied the irreversibility of such transformation (cycles involving a heating from RT up to 1075 K and then cooling from 1075 K down to RT) by means of magnetization vs temperature measurements through a series of oscillating temperature sweepings of ±100 K. The resulting curve is shown in Fig. 6 together with an approximate definition (shaded in grey) of the different regions where $M(T)$ reversibility and irreversibility are found. A complementary study, in which the sample is subjected to subsequent heating-cooling cycles, is depicted in Fig. 7. These cycles have been done as follows: the as-milled sample was heated up to 1075 K and cooling down to RT twice, in such a way that the sample displays the same behavior to that in Figs. 1 and 5. After that, the sample was subsequently heated up to three selected temperatures (on the different regions of stability of Fig. 6) and cooling down to RT after each heating [up to 675 K, Fig. 7(a); up to 875 K, Fig. 7(b); and up to 1075 K, Fig. 7(c)]. In Fig. 7 the $M(T)$ curve of Fig. 5 is plotted in gray for reference. These curves

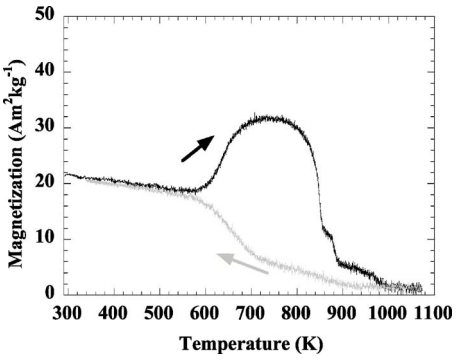

FIG. 5. Magnetization vs temperature $M(T)$ curves for the fcc-$Fe_{16}Cu_{84}$ solid solution for the second heating (black) and cooling (grey) processes.

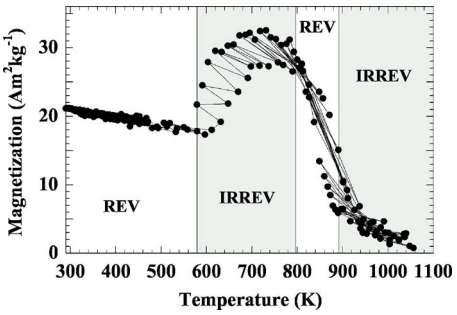

FIG. 6. $M(T)$ curve of the $Fe_{16}Cu_{84}$ after cooling from 1075 K. An oscillating temperature ramp (±100 K) has been used in order to show different zones for the reversibility (REV) and irreversibility (IRREV) of the magnetization. Thin lines are plotted between consecutive measured points.

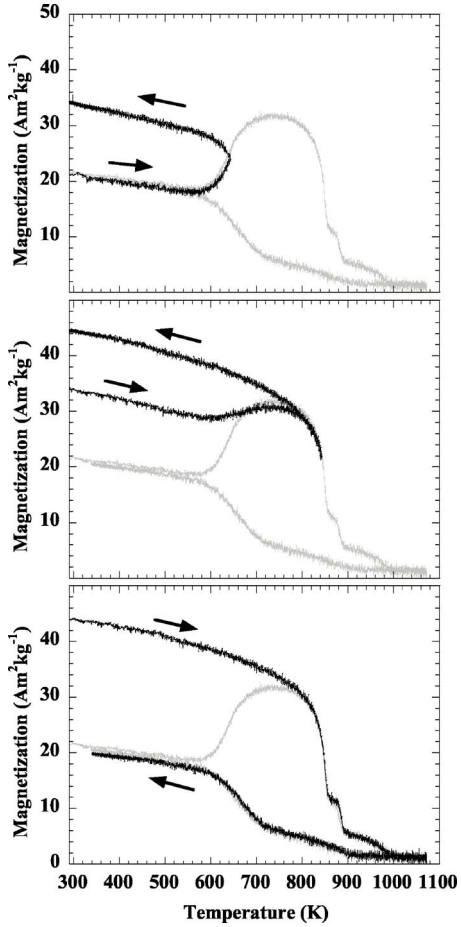

FIG. 7. Heating-cooling $M(T)$ cycles up to selected temperatures in order to show the different zones for irreversibility and reversibility of the magnetization of the fcc-$Fe_{16}Cu_{84}$. The curves are compared with the $M(T)$ curve of the segregated sample shown in Fig. 5. The arrows indicate the heating and cooling measurements.

confirm the main results obtained from Fig. 6 and define the intrinsic nature of the physical effect involved. Only when the sample temperature is raised up to 875 K do the data of the heating and cooling process retrace [cooling curve of Fig. 7(b) and heating curve of Fig. 7(c)]. Finally, when the sample is taken to 1075 K and cooled back down the results reproduce those presented in Fig. 5. In other words, the $M(T)$ curve on cooling is always the same if the MA transition is overcome. To be consistent, we have measured the magnetization on different samples from different samples from several preparation runs, testing up to four temperature cycles, finding on all the cases the same results as in Figs. 1 and 5–7.

The key question to be answered is what is the origin for the abrupt increase of magnetization around 600 K in the subsequent heating-cooling processes when the final temperature of the previous cycle is not higher than 875 K. To make further progress in understanding of this puzzling behavior, we must examine the different possible explanations.

(a) The first hypothesis to be considered is the possible effects due to significant existence of Fe oxides, which should be magnetic (thus discarding FeO). In fact depending on the nature of the oxide, the Curie or Néel temperatures vary from magnetite (Fe_3O_4) with 850 K, to 950 K in α-Fe_2O_3 (hematite), and γ-Fe_2O_3 (maghemite), close to the range where the shoulders in the magnetization data are seen. However, in the neutron-diffraction experiments we have not detected any intensity which could be associated with those oxides, before and after the temperature cycles. In any case, if the Fe oxides were under the neutron detection ($<5\%$) threshold, it is impossible that a minor quantity of the mentioned oxides (of ferromagnetic or weak ferromagnetic nature)[32] can give rise to such increase of magnetization.

(b) Perhaps at first sight the simplest explanation is to think that the segregation process observed in the first heating-cooling cycle (Fig. 1) takes place again after each temperature cycle. This will mean that the Fe and Cu single phases found at high temperatures are being reagregated in the cooling process. This possibility seems to be unlikely due to the nearly zero solubility of Fe and Cu.[33] In addition to the cell parameter $a=3.617(2)$ Å of the Cu phase obtained at RT from the Rietveld analysis of the neutron-diffraction patterns in Fig. 3(d) clearly indicates that the amount of Fe is almost zero, as it corresponds to the metallic pure Cu parameter ($a=3.615$ Å). Finally, and as we have mentioned above, if the sample is heated above 1000 K (see Fig. 5) the same $M(T)$ behavior is observed in subsequent heating and cooling processes, that is, thermomagnetization curves overlap. The latter makes very difficult to believe in a segregation reagregation of the same amount of atoms at each consecutive heating-cooling cycle.

(c) If we rule out the two above hypotheses, we have three candidates responsible for explaining the physics underlined in Figs. 5–7: bcc-Fe, fcc-Cu, and γ-Fe precipitates. Among these crystallographic phases, the only one that could originate such a high temperature magnetic instability is γ-Fe, because, as it is well known, bcc-Fe behaves as a conventional ferromagnetic material and Cu is diamagnetic. In fact, this magnetovolume instability is a rapid change of the magnetic moment with respect to a small change in the atomic volume. The observations found in the magnetization at high temperatures look remarkably similar to an anti-Invar behavior, with values of at least $2.5\mu_B$ per Fe atom for the magnetic moment.

In order to understand such striking magnetic behavior, we must remember that a temperature increase implies a lattice expansion, and, as has been proposed earlier,[4,11,13,34] the γ-Fe can exhibit anti-Invar behavior, which means that the thermal expansion coefficient has larger values (above 20×10^{-6} K^{-1}) than those for typical $3d$ metals (around $10-15\times10^{-6}$ K^{-1}).[1] The temperature dependence of the lattice parameter a (see Fig. 8) associated with the γ-Fe crystal structure allow us to estimate, through a reasonable linear fitting, the thermal expansion coefficients giving values of $21(1)\times10^{-6}$ K^{-1} (on heating) and $23(2)\times10^{-6}$ K^{-1} (on cooling). For the latter data points, the error bars are larger due to the uncontrolled variation of the temperature, giving rise to a larger temperature gradient between the sample and the temperature control reference in the oven. In both cases the values obtained for α_T are above 20×10^{-6} K^{-1}, higher than that of pure bcc-Fe (12×10^{-6} K^{-1})[1] and close to the expected values found in similar systems as FeNiMn alloys

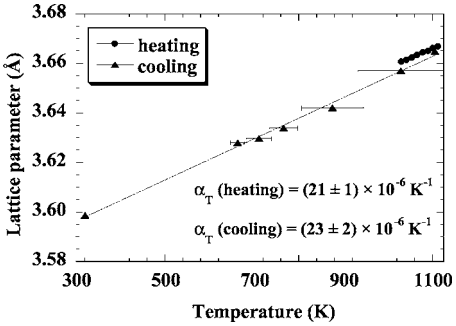

FIG. 8. Temperature dependence of the lattice parameter of γ -Fe phase on heating and cooling obtained from the Rietveld analysis of the neutron-diffraction data. Lines show a linear fits to the data.

$(21\times10^{-6}\ \mathrm{K}^{-1})$.[1,34] The explanation for these high values of the thermal expansion in γ-Fe lies on the basis of thermally activated excitations from a LS to a HS state, leading to the appearance of ferromagnetism at high temperatures, and accompanied by an extra (2–3 %)[1] increase in the lattice parameter that is superimposed on the normal lattice expansion. In our case, the lattice parameter at RT for the isolated γ-Fe phase, estimated from neutron diffraction data, is around 3.59(1) Å after cooling from 1100 K. Hence, an increase of 300 K is enough to expand the lattice to over 3.6 Å and stabilize the HS state, thus inducing ferromagnetic order in γ-Fe, with a concomitant high value of μ_{Fe}, and supporting the validity of the values of the volume fractions obtained for α- (10%) and γ-Fe (5%) which had been calculated from the neutron-diffraction data. In addition, the appearance of ferromagnetic order induces an extra volume expansion owing to a strong magnetoelastic coupling. However, how this γ-Fe phase is formed and located at likely the grain boundaries[35] remains presently unanswered. Further work will be needed in order to obtain complementary information. The existence of a magnetic anti-Invar behavior confirms the theoretical predictions of Moruzzi[11] concerning the high-temperature moment-volume instability in γ-Fe. Using total-energy band calculations it was shown that in γ-Fe and for lower electron concentration ferromagnetism could be induced at some characteristic temperature (in our case $\sim$500 K) accompanied with an enhancement of the thermal expansion coefficient (see Figs. 4 and 5 in Moruzzi's paper[11]).

On the other hand, in order to understand the irreversibility in the heating-cooling process (see Fig. 5), the fact that during heating from RT, the isolated γ-Fe precipitates are surrounded by ferromagnetic α-Fe grains which are producing a high local magnetic field.[36] Hence, this field acts as a "driving force" which contributes to the appearance of ferromagnetism in the γ-Fe. On the other hand, and during cooling from high temperature, the whole system is nonmagnetic, thus the combined effect of a different thermal expansion evolution of γ-Fe together with the absence of a high local magnetic field coming from α-Fe phase leads to such a magnetic irreversibility.

Finally, we measured also another two samples of compositions $Fe_{44}Cu_{56}$ and $Fe_{65}Cu_{35}$. Similar behavior is observed in these fcc solid solutions; a small amount of isolated γ-Fe phase coexists at RT with bcc-Fe and fcc-Cu phases after cooling from 1075 K. After the full segregation process this γ-Fe presents temperature-induced ferromagnetic order above 500 K. However, in these two samples with higher Fe content the amount of segregated bcc-Fe-rich phase is much larger, and the magnetization enhancement is less spectacular than that seen in the $Fe_{16}Cu_{84}$ alloy.

IV. SUMMARY

In conclusion, we provide experimental data revealing an anomalous high-temperature behavior of the magnetization in mechanically alloyed FeCu, which is correlated with neutron scattering data. When the as-milled Cu-rich sample is heated above 500 K, a thermal activated segregation process gives rise to a two-phase system with a bcc-Fe-rich phase ($\approx$15%) in presence of a predominant ($>$80%) fcc-Cu phase. Further heating shows an anomalous martensite-austenite transformation of the bcc-Fe phase with a large thermal hysteresis on heating-cooling cycles. In addition to that, a small amount of fcc-Fe phase ($\approx$5%) is retained during cooling from 1100 K. The formation of such isolated γ-Fe precipitates, with a high value of the coefficient of thermal expansion, seems to be responsible for the anomalous increase of the magnetization observed above 600 K in the second temperature cycle. This high-temperature magnetic instability is a consequence of magnetovolume effects in the γ-Fe phase exhibiting anti-Invar behavior. However, how this high-temperature instability is related to the local FeCu environment remains presently unanswered. Iron lattice requires a minimum value for its volume in order to exhibit ferromagnetism. If the lattice parameter reaches a value favoring a nonmagnetic or a low magnetic moment state, γ -Fe shows anti-Invar behavior during heating, with an anomalous large value for the thermal expansion. This results in the induction of ferromagnetism when the crossover to HS state takes place. On the other hand, fcc-FeCu solid solutions are found to be an ideal system to show either Invar or anti-Invar behavior in γ-Fe, because it is feasible to monitor (through composition and temperature) the formation of fcc phases which display the suitable atomic distances in between the critical values for the LS and HS states for γ-Fe. Accordingly, the FeCu solid solutions become an ideal case study to check the validity of previous theoretical models as well as "*ab initio*" band structure calculations.

ACKNOWLEDGMENTS

The work was partially supported by the Research Grants MAT2002-04178-C04, MAT2002-11621-E, MAT2003-06942, FICyT-PB02-037, and by EU under IHP program. We also thank the ISIS facility (UK) for the allocation of neutron beam time. D.M.-B. thanks the Spanish MICyT for additional support.

[1] W. Pepperhoff and M. Acet, *Constitution and Magnetism of Iron and its Alloys* (Springer, Heidelberg, 2001), Vol. 8, p. 1.
[2] S. V. Grigoriev, S. V. Maleyev, A. I. Okorokov, H. Eckerlebe, and N. H. van Dijk, Phys. Rev. B **69**, 134417 (2004).
[3] S. Khmelevskyi and P. Mohn, Phys. Rev. B **69**, 140404 (2004).
[4] V. L. Moruzzi and P. M. Marcus, in *Ferromagnetic Materials*, edited by K. H. J. Buschow (North-Holland, Amsterdam, 1993), Vol. 7, Chap. 2, p. 152.
[5] P. M. Marcus, S. L. Qiu, and V. L. Moruzzi, J. Phys.: Condens. Matter **11**, 5709 (1999).
[6] S. Khmelevskyi, I. Turek, and P. Mohn, Phys. Rev. Lett. **91**, 037201 (2003).
[7] M. Van Schilfgaarde, I. A. Abrikosov, and B. Johansson, Nature (London) **400**, 46 (1999).
[8] F. Decremps and L. Nataf, Phys. Rev. Lett. **92**, 157204 (2004).
[9] E. F. Wassermann, in *Ferromagnetic Materials*, edited by K. H. J. Buschow and E. P. Wohlfarth (North-Holland, Amsterdam, 1990), Vol. 5, Chap. 3, p. 237.
[10] R. J. Weiss, Proc. Phys. Soc. London **82**, 281 (1963).
[11] V. L. Moruzzi, Phys. Rev. B **41**, 6939 (1990).
[12] A. F. Tatarchenko, V. S. Stepanyuk, W. Hergert, P. Rennert, R. Zeller, and P. H. Dederichs, Phys. Rev. B **57**, 5213 (1998).
[13] H. C. Herper, E. Hoffmann, and P. Entel, Phys. Rev. B **60**, 3839 (1999).
[14] D. Pescia, M. Stampanoni, G. L. Bona, A. Vaterlaus, R. F. Willis, and F. Meier, Phys. Rev. Lett. **58**, 2126 (1987).
[15] P. A. Montano, G. W. Fernando, B. R. Cooper, E. R. Moog, H. M. Naik, S. D. Bader, Y. C. Lee, Y. N. Darici, H. Min, and J. Marcano, Phys. Rev. Lett. **59**, 1041 (1987).
[16] A. R. Yavari, P. J. Desré, and T. Benameur, Phys. Rev. Lett. **68**, 2235 (1992).
[17] A. Hernando, P. Crespo, A. García Escorial, and J. M. Barandiarán, Phys. Rev. Lett. **70**, 3521 (1993).
[18] J. Eckert, J. C. Holzer, and W. L. Johnson, J. Appl. Phys. **73**, 131 (1993).
[19] C. L. Chien, S. H. Liou, D. Kofalt, Wu Yu, T. Egami, and T. R. McGuire, Phys. Rev. B **33**, 3247 (1986).
[20] E. Ma, M. Atzmon, and F. E. Pinkerton, J. Appl. Phys. **74**, 955 (1993).
[21] V. G. Harris, K. M. Kemner, B. N. Das, N. C. Koon, A. E. Ehrlich, J. P. Kirkland, J. C. Woicik, P. Crespo, A. Hernando, and A. García Escorial, Phys. Rev. B **54**, 6929 (1996).
[22] P. Gorria, D. Martínez-Blanco, J. A. Blanco, A. Hernando, J. S. Garitaonandia, L. Fernández Barquín, J. Campo, and R. I. Smith, Phys. Rev. B **69**, 214421 (2004).
[23] W. A. A. Macedo and W. Keune, Phys. Rev. Lett. **61**, 475 (1988).
[24] J. Z. Jiang, Q. A. Pankhurst, C. E. Johnson, C. Gente, and R. Bormann, J. Phys.: Condens. Matter **6**, L227 (1994).
[25] G. Mazzone and M. Vittori Antisari, Phys. Rev. B **54**, 441 (1996).
[26] P. Crespo, A. Hernando, R. Yavari, O. Drbohlav, A. García Escorial, J. M. Barandiarán, and I. Orue, Phys. Rev. B **48**, 7134 (1993).
[27] M. Eilon, J. Ding, and R. Street, J. Phys.: Condens. Matter **7**, 4921 (1995).
[28] J. Rodríguez-Carvajal, Physica B **192**, 55 (1993).
[29] *Magnetic Properties of Metals, d-elements, Alloys and Compounds*, edited by H. P. J. Wijn (Springer-Verlag, Berlin, 1991), p. 22.
[30] D. H. Ucko, Q. A. Panckhurst, L. Fernández Barquín, J. Rodríguez Fernández, and S. F. J. Cox, Phys. Rev. B **64**, 104433 (2001).
[31] P. Crespo, N. Menéndez, J. D. Tornero, M. J. Barro, J. M. Barandiarán, A. García Escorial, and A. Hernando, Acta Mater. **46**, 4161 (1998).
[32] E. Murad, Hyperfine Interact. **111**, 251 (1998).
[33] L. J. Swartzendruber, in *Binary Alloy Phase Diagrams*, 2nd ed., edited by T. B. Massalski (ASM International, Ohio, 1990), Vol. 2, p. 1408.
[34] M. Acet, H. Zähres, E. F. Wassermann, and W. Pepperhoff, Phys. Rev. B **49**, 6012 (1994).
[35] A. Hernando, P. Crespo, A. García Escorial, J. M. Barandiarán, M. Urchulutegui, and M. Vittori Antisari, Europhys. Lett. **32**, 585 (1995).
[36] A. Hernando, I. Navarro, and P. Gorria, Phys. Rev. B **51**, R3281 (1995).